OPEN ACCESS

Super phase array

To cite this article: W H Wee and J B Pendry 2010 *New J. Phys.* **12** 033047

New Journal of Physics
The open-access journal for physics

Super phase array

W H Wee[1] **and J B Pendry**
Condensed Matter Theory Group, Department of Physics,
Imperial College London, London SW7 2AZ, UK
E-mail: w.wee07@imperial.ac.uk

New Journal of Physics **12** (2010) 033047 (15pp)
Received 5 November 2009
Published 24 March 2010
Online at http://www.njp.org/
doi:10.1088/1367-2630/12/3/033047

Abstract. For a long time, phase arrays have been used in a variety of wave transmission applications because of their simplicity and versatility. Conventionally, there is a trade-off between the compactness of a phase array and its directivity. In this paper, we demonstrate how by embedding a normal phase array within a superlens (made of negative refractive index material) we can overcome this constraint, and create compact phase arrays with a virtual extent much larger than the physical size of the array. In this paper, we also briefly discuss the apparent unphysical field divergences in superlenses, and how to resolve this issue.

[1] Author to whom any correspondence should be addressed.

Contents

1. Introduction **2**
2. Super phase array **3**
2.1. How to create a super phase array 3
2.2. N-array and beam forming 4
3. Analytical model **6**
3.1. Addition theorem 6
3.2. Transfer matrices 7
3.3. Resolving divergences 9
4. Results **10**
4.1. Single displaced antenna 10
4.2. N-array antenna 12
5. Conclusion **14**
Appendix **14**
References **15**

1. Introduction

A phase array is a group of transmitters in which the relative phases of the respective signals feeding the transmitters are varied in such a way that the effective radiation pattern of the array is reinforced in a desired direction and suppressed in undesired directions. The phase array has a long history, and was first developed by Karl Ferdinand Braun in 1905, when he demonstrated that a phase array has an enhanced transmission of radio waves in one direction. By varying the relative phases of the phase array antennas, one can also electronically steer (without any mechanical moving parts) a radiating beam rapidly in a desired direction. This was exploited by Luis Alvarez during World War II, when he used a phase array antenna to create a rapidly steerable radar system to aid the landing of airplanes in England. Owing to its versatility and simplicity, even now the phase array has a wide variety of modern military, commercial and research applications.

The principle of the phase array antenna comes from the Huygens principle, where an advancing wavefront can be regarded as a sum of contributions from an infinite set of radiating points preceding the wavefront. This means that if we have an infinite extent of transmitters spaced at sub-wavelength intervals and if we can adjust the phase and amplitude of each transmitter, we can, in principle, recreate any wavefront. In practice we can relax the condition of an infinite extent of radiating transmitters, but the cost of having a finite extent of transmitters is the loss of directivity. In general, the larger the extent (aperture size) of the transmitters, the greater the directivity, hence a compromise between the physical extent and the directivity of a phase array.

In [1, 2], we have demonstrated that by using a suitable negative refractive index material (NRIM) we can create super-scatterers (SSs) [3]—scatterers with a scattering cross section much larger than the physical dimension of the scatterer. Here we hope to extend the ideas introduced in [2] to create a super phase array—a phase array with an apparent size much larger

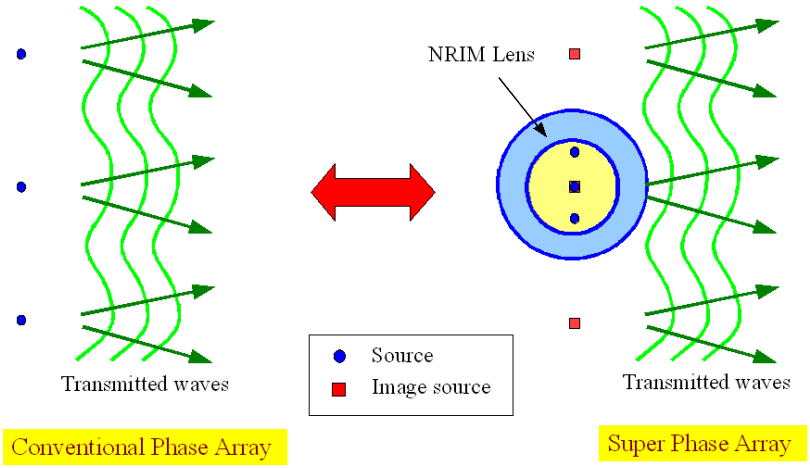

Figure 1. A conventional phase array can, in principle, recreate any wavefront when each transmitter of the array is radiating at the right amplitude and phase. A smaller super phase array can emulate a physically larger conventional phase array by amplifying the evanescent optical modes.

than its physical dimension, and hence more compact than any conventional phase array—yet without the loss of directivity (see figure 1).

With this intent, the paper is divided into the following three sections. Firstly, in section 2, we discuss how we can create a super phase array, and how we can achieve beam forming using an N-array phase array. Following this in section 3, we discuss the analytical methods used to study the super phase array. Finally in section 4, we apply the methods from section 3 to study the effects of losses, and show some numerical simulations of beam forming using a super phase array.

2. Super phase array

2.1. How to create a super phase array

Basically, if we embed a conventional phase array in a transparent SS [2] (transparent SS) we get a super phase array. What is a transparent SS? A transparent SS is a scatterer that compactifies a region of transparent space[2] to a smaller region within the scatterer. Conversely, this implies that any object (scatterers/transmitters) placed within the transparent SS would appear larger by the degree of compaction (see figure 1). To illustrate the principles, we focus only on a specific case of the cylindrically symmetric transparent SS in this paper. We can easily generalize this to other geometry by using transformation optics [4]–[7].

The permittivity and permeability ($\boldsymbol{\epsilon}$ and $\boldsymbol{\mu}$, respectively) for a cylindrical transparent SS is given by

$$\boldsymbol{\epsilon_I} = \boldsymbol{\mu_I} = \mathrm{diag}\left[\epsilon_x^{(I)}, \epsilon_y^{(I)}, \epsilon_z^{(I)}\right], \quad r_{I-1} < r \leqslant r_I, \tag{1}$$

[2] This region may or may not be surrounding the transparent SS.

where the index $I = 1, 2, 3$ denotes the three main regions of the transparent SS (region I is defined by $r_{I+1} < r \leqslant r_I$) and

$$\begin{aligned} &\epsilon_x^{(1)} = +1, \quad \epsilon_y^{(1)} = +1, \quad \epsilon_z^{(1)} = +1, \quad r_2 < r \leqslant r_1, \\ &\epsilon_x^{(2)} = -1, \quad \epsilon_y^{(2)} = -1, \quad \epsilon_z^{(2)} = -\frac{r_2^4}{r^4}, \quad r_3 < r \leqslant r_2, \\ &\epsilon_x^{(3)} = +1, \quad \epsilon_y^{(3)} = +1, \quad \epsilon_z^{(3)} = +\frac{r_2^4}{r_3^4}, \quad r \leqslant r_3, \end{aligned} \tag{2}$$

where region 1 is the vacuum surrounding the transparent SS (given by $r_2 < r \leqslant r_1$, where $r_1 = r_2^2/r_3$), region 2 is the NRIM layer (r_2 and r_3 are the outer and inner radii of the NRIM annulus), which is designed to optically cancel[3] out region 1, and region 3 is the interior region of the transparent SS, designed such that it is optically equivalent to vacuum of radius r_1.

When the NRIM layer optically cancels the surrounding vacuum, the resulting image of region 3 is magnified to fill up the canceled regions. Effectively such a transparent SS then behaves like a magnifying glass—a superlens [1], [8]–[10]—such that objects within are magnified by a factor of $r_1/r_3 = r_2^2/r_3^2$. What is remarkable is that any object with a radius larger than r_3^2/r_2 would cast an image larger than the physical size of the lens ($>r_2$), something that cannot be achieved by a conventional lens. The reason why this is so is because conventional optics work by manipulating only the propagating far-fields. An NRIM lens can capture both the propagating far-fields and the evanescent near-fields (through resonances in the lens).

This implies that if we embed a phase array within such a lens, the array would appear to be larger by a factor of r_1/r_3. In addition, if the phase array has a size larger than r_3^2/r_2, then the image of the phase array would appear to be larger than the physical size of the setup.

Now before we proceed to the next section, it is interesting to note that the material parameters for the superlens given by (2) can be relaxed/simplified in the quasi-static limit—that is when all length scales (the dimensions of the super phase array, and the distance that the detector is placed) are smaller than the wavelength of radiation ($l \ll \omega c$), we can decouple the E and H fields, so that the scattering of p-polarization (s-polarization) waves depends solely on spatial variations of $\boldsymbol{\epsilon}$ ($\boldsymbol{\mu}$) alone [8]. This means that for antennas radiating only p-polarization, and if we are only interested in measurement of the near fields, we can simplify the superlens structure by ignoring $\boldsymbol{\mu}$ setting $\mu_x^{(2)} = \mu_y^{(2)} = \mu_z^{(2)} = 1$ and $\epsilon_x^{(2)} = \epsilon_y^{(2)} = \epsilon_z^{(2)} = -1$ (similarly for s-polarization). This simplification for instance was exploited by [11]–[13] to create a 'poor man's' cylindrical superlens for use in external cloaking.

2.2. N-array and beam forming

Having seen how to create a super phase array, we shall now briefly discuss how phase arrays in general transmit radiation of a desired pattern—beam forming. By varying the amplitude and the phase of the input for each transmitter in the phase array, we can reshape the transmitted wavefront in any manner we desire. In this paper, we will explore two specific examples of such beam forming using the super phase array—beam steering and beam focusing.

Firstly, consider a linear phase array with N evenly distributed transmitters (let N be an odd number). Let each transmitter be labeled $n = 1$ to N, and let each transmitter be separated

[3] This optical cancelation can be understood as the phase and amplitude reversal of a wave when it passes from one medium to its optical complementary. This is true for both the propagating and evanescent waves.

by a distance r_0. We note that for the phase array to work $r_0 < \lambda$, where λ is the wavelength of the transmitted wave in the medium that the phase array is embedded in. Transmitters that are spaced larger than the wavelength apart will interfere nontrivially in the far field.

Suppose the linear array lies along the x-axis, with the center of the array ($n = (N-1)/2$) at the origin ($x = y = 0$). If we want to recreate a wavefront that has the following field amplitude $\Psi(x, y)\exp(-i\omega t)$ (propagating in the y-direction), we can do so when the signal input for the nth transmitter is given by

$$\Psi_n = \int \Psi(x, y = 0) \cdot \delta(x - n \cdot r_0)\, dx. \tag{3}$$

For simplicity, in this paper we assume that $\Psi_n = 1$. Now we can add a further refinement to the phase array when we allow the signal input, $\tilde{I}_n$, for the nth transmitter in the array to be given by

$$\tilde{I}_n = \left[A_n \cdot \exp(-i\phi_n)\right] \cdot \Psi_n, \tag{4}$$

where A_n is the aperture function while ϕ_n dictates the additional phase to be added to the transmitted wave. To suppress side lobes due to a finite extent of the array, we need to choose an aperture function with a smoother cut-off. For this reason, we choose the following aperture function with a Gaussian envelope:

$$A_n = \exp\left[-\left(\frac{(n - (N-1)/2) \cdot r_0}{w_0}\right)^2\right], \tag{5}$$

where the Gaussian envelope is centered at the $(N-1)/2$ transmitter and w_0 is the width of the Gaussian envelope. Here in this paper we choose $w_0 = (N-1)/2 \cdot r_0$.

Now by applying a linear phase delay to each transmitter in the phase array (assuming the transmitters are equally spaced), we can tilt a wavefront while preserving its shape. That is, if ϕ_n is given by

$$\phi_n = k \cdot n \cdot r_0 \sin(\alpha), \tag{6}$$

where k is the wave vector of the transmitted wave in the medium that the array is embedded in, then the wavefront can be tilted by an angle α (where $\alpha = 0$ lies in the perpendicular direction to the linear phase array), thus achieving beam steering.

Now other than beam steering, we can demonstrate beam focusing by applying a parabolic phase shift to the array, such that ϕ_n is given by

$$\phi_n = k\left[\sqrt{((n - (N-1)/2) \cdot r_0)^2 + f^2} - f^2\right], \tag{7}$$

where f is the distance from the center of the array that the beam would focus at. For $f \gg N \cdot r_0$ the phase ϕ_n from (7) can be simplified as

$$\phi_n \approx \frac{k}{2f} \cdot ((n - (N-1)/2) \cdot r_0)^2. \tag{8}$$

When we substitute (5) and (8) into (4), the resulting beam profile compares closely with the initial value of the theoretical 2D Gaussian beam, and the resultant wave propagation problem can be compared with the theoretical 2D Gaussian beam propagation. In section 4 of the paper, we shall demonstrate the use of the super phase array to beam steer and beam focus.

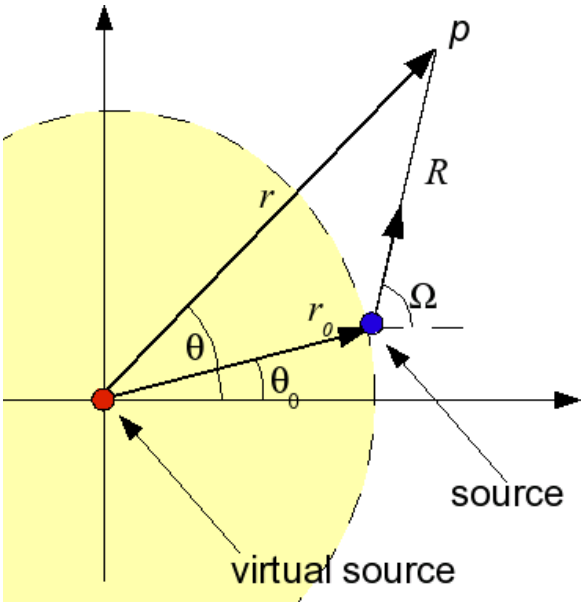

Figure 2. Illustration of the addition theorem. We can create the fields of a displaced source by placing an infinite series of virtual sources at the origin.

3. Analytical model

Having seen from section 2 how one can create a super phase array, and having briefly discussed how we can achieve beam forming with a suitable input to the phase array, we shall now discuss the analytical methods that we use to model such a super phase array.

3.1. Addition theorem

First, to model the radiation from a transmitting phase array embedded in a cylindrically symmetric transparent SS, it is wise to decompose the transmitted wave into a series of cylindrical waves (which respect the cylindrical symmetry of the lens). Initially this may seem to be a futile task since a linear phase array clearly breaks the cylindrical symmetry of the problem. This, however, can be circumvented when we make use of the addition theorem [14] to displace the non-centric transmitters to the origin, thus restoring cylindrical symmetry of the problem. By displacing or relocating all the transmitting sources to the origin, we can then make use of the result from the paper [2] to determine the exact field solutions of a super phase array.

Now, suppose we have a point source with angular coordinates (r_0, θ_0), which emits cylindrical waves of angular order v (Hankel function of the first kind of order v). According to the addition theorem, we can recreate the displaced point source by placing an infinite number of point sources (with all angular orders) at $r = 0$ (see figure 2) given by

$$H_v^{(1)}(kR)\,\mathrm{e}^{\mathrm{i}v(\Omega-\theta_0)} = \sum_{m=-\infty}^{\infty} J_m(kr_0)H_{v+m}^{(1)}(kr)\,\mathrm{e}^{\mathrm{i}(v+m)(\theta-\theta_0)}\ r > r_0, \tag{9}$$

where the left-hand side of (9) is the outgoing cylindrical wave centered at (r_0, θ_0), and the right-hand side is the outgoing wave for an infinite series of sources (of all angular orders) centered at the origin, weighted by some Bessel function $J_m(kr_0)$.

In this paper, we shall assume the sources in the phase array to be simple dipoles aligned along the axial direction, so all the transmitting sources have angular order $v = 0$. Now we note that the field for a single displaced source (at (r_0, θ_0)) or an infinite series of sources located at the origin are exactly identical for $r > r_0$, but for the latter the field diverges for $r < r_0$. This has some physical implications for the superlens, in that the (perfect) image of this divergent region is also divergent, even though the region of space where the image sits on does not contain any divergent sources. This poses a problem since such an unphysical situation is impossible; it therefore implies that a superlens cannot exist in the first place. Fortunately, this problem can be resolved and we address this problem in section 3.3.

3.2. Transfer matrices

Since the problem we have set out with is essentially 2D, we only need concern ourselves with TE polarization, and the solution of the electric field vector only lies along the axial direction (z-axis). The solution for the electric field vector is given by $E_z^{(I)}(r, \phi)$, where the superscript denotes the region, according to the definition from (2). According to the discussion of our previous paper [2], the field solutions for the various regions in the transparent SS are then given by the following:

$$E_z^{(1)} = E_{z0} \sum_{m=-\infty}^{m=\infty} \left[d_m H_m^{(1)}(k_1 r) \right] \mathrm{i}^m \mathrm{e}^{(\mathrm{i}m\phi - \mathrm{i}\omega t)}, \quad r \geqslant r_2, \tag{10}$$

$$E_z^{(2)} = E_{z0} \sum_{m=-\infty}^{m=\infty} \left[b_m H_m^{(1)}\left(k_2 \left[\frac{r_2^2}{r}\right]\right) + c_m J_m\left(k_2 \left[\frac{r_2^2}{r}\right]\right) \right] \mathrm{i}^m \mathrm{e}^{(\mathrm{i}m\phi - \mathrm{i}\omega t)}, \quad r_3 \leqslant r \leqslant r_2, \tag{11}$$

$$E_z^{(3)} = E_{z0} \sum_{m=-\infty}^{m=\infty} \left[I_m H_m^{(1)}(k_3 r) + a_m J_m(k_3 r) \right] \mathrm{i}^m \mathrm{e}^{(\mathrm{i}m\phi - \mathrm{i}\omega t)}, \quad r \leqslant r_3. \tag{12}$$

With the wave vectors in (10)–(12) given by

$$\begin{aligned} k_1 &= \omega/c, \\ k_2 &= (1 - \mathrm{i}\delta) k_1, \\ k_3 &= \left(\frac{r_2}{r_3}\right)^2 k_1, \end{aligned} \tag{13}$$

where δ is the loss tangent—a measure of losses in the NRIM layer of the transparent SS.

I_m, b_m, d_m and a_m, c_m of (10)–(12) are the *scattering coefficients* of the outgoing and incoming cylindrical waves, respectively. Except for I_m, all the other coefficients are unknown and, when they are determined, would give the exact field solution to the problem. The coefficient I_m is dependent on the configuration and the signal input of the phase array. Using the addition theorem from (9), we can shift all the transmitters to the origin. Together with the signal input $\tilde{I}_n$ (from (4)) for the nth transmitter of the array, this would give us

$$I_m = \sum_{n=0}^{N} \tilde{I}_n J_m(k_3 r_n) \exp(\mathrm{i}m\theta_n), \tag{14}$$

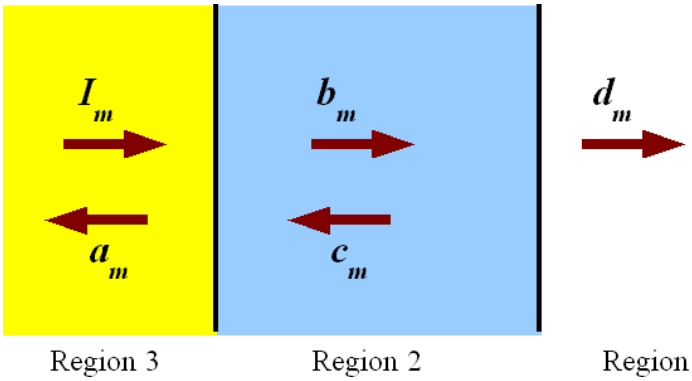

Figure 3. By matching boundary conditions at the interface, we can determine the field amplitudes for each cylindrical wave mode of order m.

where (r_n, θ_n) are the position vectors of the nth transmitter. For our particular configuration—the linear phase array—these are given by

$$r_n = \left(n - \frac{(N-1)}{2}\right) \cdot r_0, \tag{15}$$

$$\theta_n = \left(1 - \Theta\left(n - \frac{(N-1)}{2}\right)\right) \cdot \pi. \tag{16}$$

Now we can determine the remaining four unknown scattering coefficients by matching the boundary conditions at the interface of each region (see figure 3), namely that the tangential E and H field vectors projected onto the surface of the interface have to be continuous, that is

$$\begin{aligned} \mathbf{E}_{\parallel}^{(I)}(\mathbf{r}) &= \mathbf{E}_{\parallel}^{(I+1)}(\mathbf{r}), \quad I = 1, 2, \\ \mathbf{H}_{\parallel}^{(I)}(\mathbf{r}) &= \mathbf{H}_{\parallel}^{(I+1)}(\mathbf{r}), \quad I = 1, 2, \end{aligned} \tag{17}$$

where explicitly for our case

$$\begin{aligned} \mathbf{E}_{\parallel}^{(I)} &= E_z^{(I)}\hat{\mathbf{z}}, \\ \mathbf{H}_{\parallel}^{(I)} &= H_{\phi}^{(I)}\hat{\boldsymbol{\phi}} = \frac{-\mathrm{i}}{\mu_{\phi}\mu_0 w} \cdot \frac{\partial}{\partial r} E_z^{(I)}\hat{\boldsymbol{\phi}}. \end{aligned} \tag{18}$$

Substituting (10)–(12) into the boundary conditions (17), we can then solve the remaining unknown scattering coefficients (see appendix). As expected, when there are no losses in the NRIM ($\delta = 0$), we would get no reflections ($a_m = c_m = 0$) and all the waves would be transmitted without loss ($b_m = d_m = I_m$) (see (A.1)). It is also important to note that since $k_3 r_n = k_1[(r_2^2/r_3^2) \cdot r_n]$ (according to (13)), the argument in I_m in (14) for fields in region 3 is the same as that for fields in region 1. This, together with the fact that for the lossless case, the scattering coefficients in both regions are the same, implies that the functional forms of the fields according to (10) and (12) are the same—except that the array when viewed from the outside (region 1) appears to be magnified by a factor of r_2^2/r_3^2 compared to the inside (region 3).

Hence for the lossless case, we can reverse the addition theorem, and see that the size of the virtual image of the array would be the same as that of the embedded array, magnified by a factor of r_2^2/r_3^2, as discussed previously.

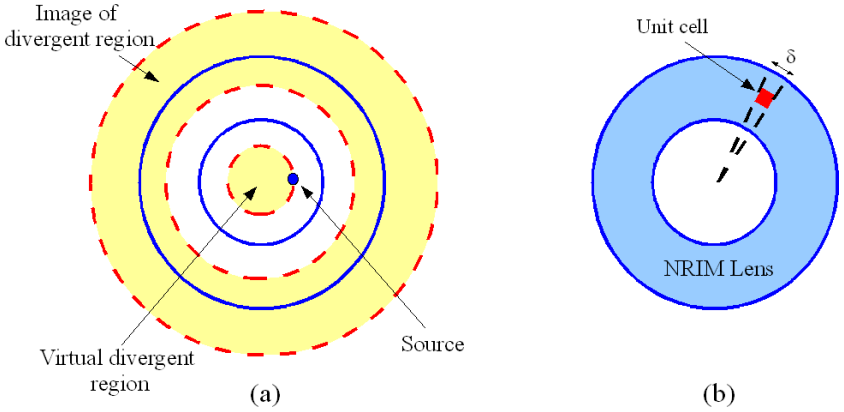

Figure 4. (a) Illustration of the problem of field divergence for a perfectly homogeneous NRIM lens. This problem of divergence can be accounted for since all real materials have losses or have a finite length scale where the homogeneity of the NRIM breaks down as shown in (b).

3.3. Resolving divergences

The perfect lens theorem [1] tells us that the field within a medium (say PRIM[4]) is a mirror image (in some planar coordinates) to its complementary (say NRIM). This means that if we know what the field solution is like for a PRIM, we can immediately write down the field solution for its complementary by reflection. Now the perfect lens theorem only holds true when there are no sources in between the two media. If we have any sources between, we need to translate these sources (for instance, via the addition theorem from section 3.1) outside the region of interest before we can apply the perfect lens theorem. Thus when we have a non-centric source in a cylindrical perfect lens, we need to relocate the source to the origin in order to determine the fields in the NRIM layer. This relocation, according to the addition theorem, would create a virtual region of divergent fields and this virtual region would in turn cast a divergent image as illustrated in figure 4(a).

This divergence in the image region now is not merely a numerical construct, but physically present, implying that it is not physically possible for a homogeneous NRIM to exist in the first place. In a similar argument, others have disputed the existence of a homogeneous NRIM [15]. It should also be noted that the exact solutions for the asymptotic behavior of these divergences are discussed in [16, 17].

This apparent paradox, however, can be accounted for by limiting the divergence in (9) through (i) imposing a higher angular momentum cut-off, (ii) imposing losses in the NRIM and (iii) considering a finite time interval in the measurement of fields. First, the source of the divergence is due to the higher angular order terms in (9). These terms, however, do not contribute to the divergence in the image region because of the following reasons:

(i) Higher angular momentum cut-off: all real materials are inhomogeneous at some length scale. So for an NRIM, the length scale at which we would see this inhomogeneity is about the size δ of the individual meta-particles (say split ring resonators etc). Now the 'perfect lensing' abilities of an NRIM assume that the NRIM is homogeneous; therefore,

[4] Positive refractive index material, or a right-handed material.

the perfect lens theorem does not apply when field fluctuations are at a length scale $\eta < \delta$. For a cylindrical wave of angular order v, and a meta-particle at a radial distance r_m, the length scale of field fluctuation near the meta-particle is given by $\eta \approx 2\pi \cdot r_m/v$. This means that any cylindrical wave with angular order $v > v_h$ (where $v_h = 2\pi \cdot r_m/\delta$) would not see the perfect lens, and hence would not contribute to the infinite series in (9), curtailing the divergence.

(ii) Losses in NRIM: an NRIM generally requires permittivity/permeability, $\epsilon, \mu < 0$. Since the energy density of electromagnetic fields in any medium must be positive, this means that $\partial(\omega\epsilon)/\partial\omega, \partial(\omega\mu)/\partial\omega > 0$. This in turn implies that if NRIM exists, it would be highly dispersive. It is also necessary then, by the Kramers Kronig relation, that a passive NRIM is also lossy. Now the higher angular order cylindrical waves present in the NRIM material are more affected by losses; thus losses in the NRIM would naturally impose a higher angular momentum cut-off to the series in (9).

(iii) Finite time interval: generally NRIM works on the principle of resonance, and these resonances take time to be established [18]; hence the perfect lens scenario strictly holds true only when $t \to \infty$. In general, the higher angular order terms of the excitation field take a longer time to be established. Hence even in the case where there are no inhomogeneities/losses, the higher angular order terms will only contribute to the image as $t \to \infty$. For finite time intervals therefore, we would not see this divergence.

4. Results

Now applying the analytical methods introduced in section 3, we can construct simulations of the super phase array and examine how losses in general affect the performance of such an array. Firstly, to understand how losses affect a general super phase array, we study how losses affect a single displaced antenna within a transparent SS in section 4.1. Following that in section 4.2, we demonstrate the performance of a super phase array in beam tilting and beam forming in comparison with a normal phase array.

4.1. Single displaced antenna

Generally, a transmitter placed at $(x_0, 0)$ within a transparent SS would create an image/impression of a virtual transmitter at $(x_{\text{image}}, 0)$ (where $x_{\text{image}} = r_2^2/r_3^2 \cdot x_0$). This means that if a transmitter is placed at distances $x_0 > r_3^2/r_2$, then the image would exist outside the physical structure of the super phase array. This result is clearly shown in figure 5. Figures 5(a) and (c) are the ray solutions, while figures 5(b) and (d) are the full wave solutions for transmitters placed at $x_0 > r_3^2/r_2$ and $x_0 < r_3^2/r_2$, respectively.

It is instructive to take note of the ray diagram for $x_0 > r_3^2/r_2$ (5(a)). Here we can see that there are two types of rays emitting from the source: blue rays and red + green rays [2]. Blue rays (called *impact rays*) impact the NRIM layer and get refracted by it through the conventional Snell's law. Red + green rays are more interesting and are called *non-impact rays*. The red self-closed loops are localized resonant optical modes in the NRIM layer, which are evanescently coupled to the green rays—rays that do not impact the superlens at all. In general, the smaller (red) self-closed loops are coupled to non-impact (green) rays with a larger impact parameter. Now, because the smaller self-closed loops are coupled to non-impact rays that are further away,

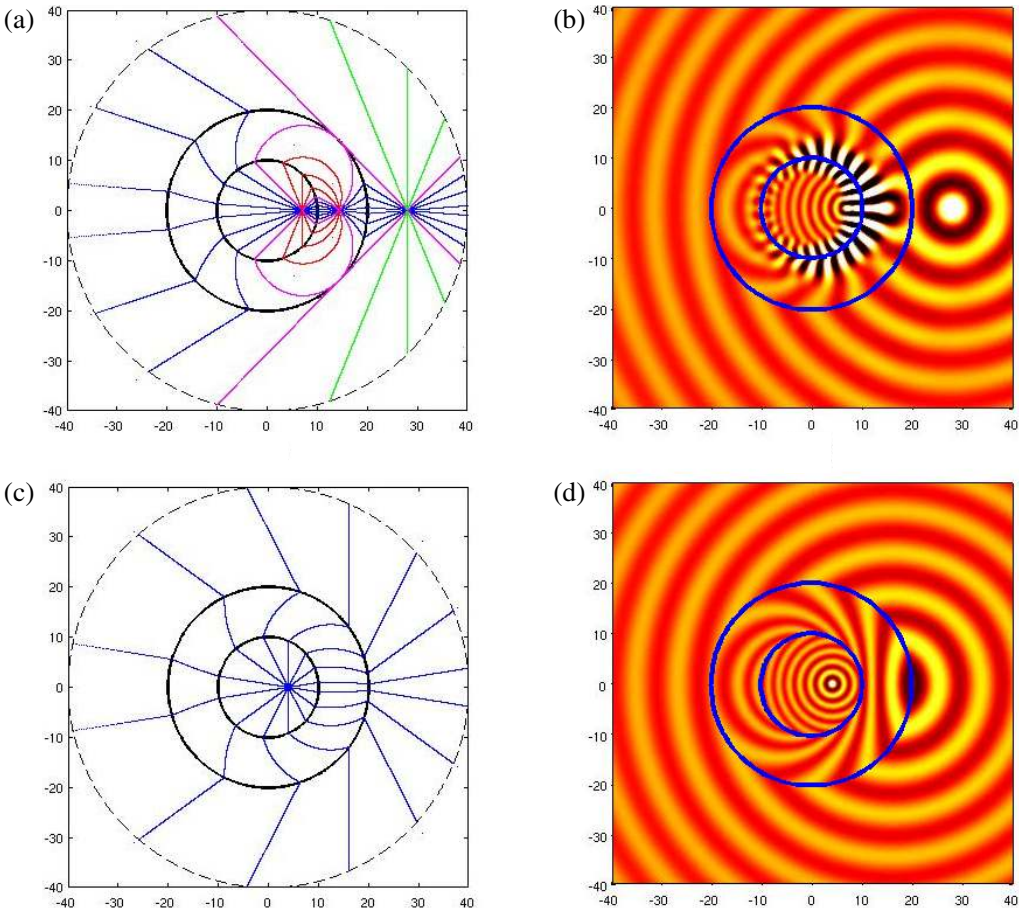

Figure 5. Parts (a) and (b) show the ray and full wave solution, respectively, of a single antenna displaced by $x = x_0 = 7$, $y = 0$ from the origin. Similarly, (c) and (d) show the ray and wave solution for $x = x_0 = 4$, $y = 0$. The outer and inner radii of the NRIM are $r_2 = 20$ and $r_3 = 10$. For (a) and (c), the blue and magenta rays are impact rays, while the red and green rays are non-impact ones.

the coupling strengths for these loops are weaker than for larger loops. Hence, any losses in the NRIM layer would therefore destroy the coupling of the smaller self-closed loops first before the larger ones.

In general then, impact rays are even more robust than non-impact rays to losses, and non-impact rays with smaller impact parameters are more robust than larger ones.

This can be clearly seen in figure 6. Figures 6(a) and (b) are plots for the field amplitude $|E_z|$ as a function of x at a distance $y = 28.75$ for a single antenna. These correspond to the same values of x_0 as in figures 5(a) and (c), respectively. From figure 6(a), we can clearly see that as losses increase, the field strength $|E_z|$ for rays with larger impact parameter decay first, and this corresponds to a dip in $|E_z|$ centered at $x = r_2^2/r_3^2 \cdot x_0$ (the position of the largest impact parameter). Eventually with sufficient losses, all the evanescently coupled non-impact rays are killed, leaving only the impact rays. From figure 6(b), since all rays are impact rays, this configuration is more robust to losses, and we do not see any dip in $|E_z|$.

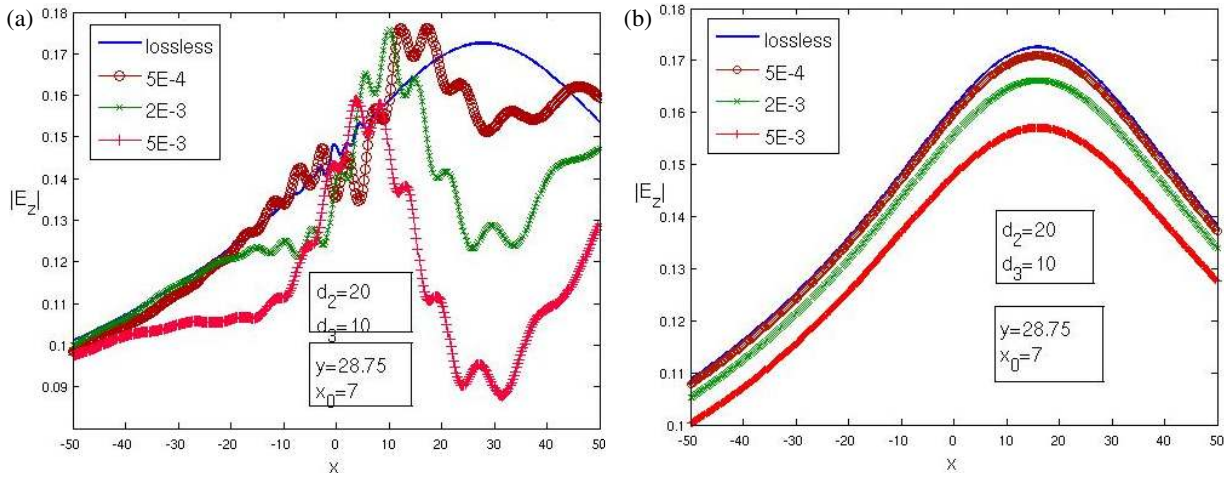

Figure 6. Parts (a) and (b) show the field amplitude $|E_z|$ as a function of x at a distance $y = 28.75$, for a single antenna displaced at $x = x_0 = 7$, $y = 0$ and $x = x_0 = 4$, $y = 0$ units away from the origin.

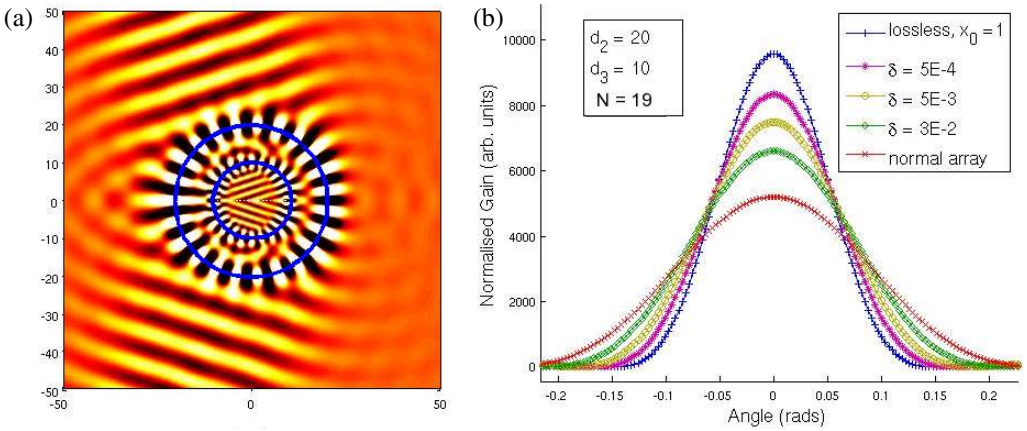

Figure 7. (a) The contour plot of an $N = 19$ array with each element separated by $r_0 = 1$ and the signal input to each with a linear phase shift (given by (6)) such that a planar waveform is tilted at angle $\alpha = \pi/10$. The outer and inner radii of the NRIM are $r_2 = 20$, and $r_3 = 10$, and losses are $\delta = 5 \times 10^{-4}$. (b) How the gain of the same setup is affected by losses.

4.2. N-array antenna

Having seen the effects of losses—that they affect non-impact rays (with larger impact parameters) more than non-impact rays—we can now understand how losses in general affect super phase arrays. In this section, we demonstrate the ability of an N-array super phase array to beam steer and beam focus, and we demonstrate how even with losses, they can outperform a conventional phase array.

4.2.1. Beam steering. Figure 7(a) shows the contour plot of an $N = 19$ super phase array with each element separated by $r_0 = 1$. The signal input is given a linear phase shift according to (6)

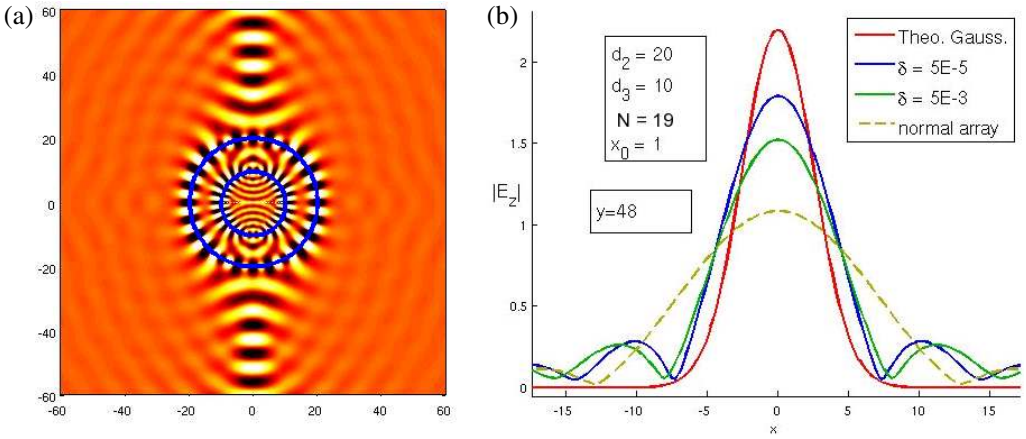

Figure 8. (a) The contour plot of an $N = 19$ array with each element separated by $r_0 = 1$ and the signal input to each with a near-parabolic phase shift (given by (7)) such that a focus is created at $f_0 = 48$. The outer and inner radii of the NRIM are $r_2 = 20$ and $r_3 = 10$, and losses are $\delta = 5 \times 10^{-4}$. (b) How the field amplitude $|E_z|$ at the focus is affected by losses.

such that the beam is tilted by $\alpha = \pi/10$. Now the outer and inner radii of the NRIM are $r_2 = 20$ and $r_3 = 10$, so this means that for a perfectly lossless NRIM, the super phase array has a physical size of $d = 2 \cdot r_2 = 40$, but a virtual size of $d_{\text{virtual}} = r_2^2/r_3^2 \cdot N \cdot r_0 = 76 > d$—about twice the physical extent.

Now since the directivity (inverse of angular spread) is proportional to the extent of the phase array, a super phase array would have a directivity d_{virtual}/d better than a normal phase array with the same physical extent. Indeed when we look at the gain of our super phase array (see figure 7(b)), we can clearly see that a lossless super phase array has a directivity about twice that of a normal phase array (with a physical extent of $d = 40$). As we have discussed, we would expect that with increasing losses, the virtual extent of the super phase array would decrease and, as expected, we see that the directivity of the super phase array drops correspondingly. Still, even with a moderate amount of losses at $\delta = 3 \times 10^{-2}$ the directivity of a lossy super phase array still outperforms that of a normal phase array.

4.2.2. Beam focusing. Now when we apply a near-parabolic phase shift according to (7), we would expect the super phase array to focus to a spot a distance $f_0 = r_2^2/r_3^2 \cdot f$ units away. In figure 8(a), we can see the super phase array (with losses $\delta = 5 \times 10^{-4}$) focusing light to a tight spot at $x = 0$, $y = f_0 = 48$.

Now the focusing power (the inverse of the angular spread) of a phase array is again proportional to the extent of the array, so we would expect the focal size of our super phase array to be d_{virtual}/d smaller than a normal phase array with the same physical extent. Indeed if we examine the field strength at the focus, $|E_z|$, as a function of x (see figure 8), we can see that a slightly lossy super phase array ($\delta = 5 \times 10^{-5}$) has about twice the focusing power than a normal phase array. Again with increasing losses, the performance of a super phase array, as we would expect, drops.

5. Conclusion

We have demonstrated how one can create a super phase array by embedding a normal phase array within a transparent SS, and how by varying the signal input to the phase array, we can alter the radiation pattern—in particular beam tilting and beam forming. In this paper, although we study the specific example of a cylindrically symmetric super phase array, the ideas can be easily extended to other geometries. We have also outlined a simple analytical procedure to study the full wave solution of the super phase array, by using the addition theorem, to translate the non-cylindrically symmetric phase array to a cylindrically symmetric one. Through the addition theorem, and the perfect lens theorem, we have also shown the potential problem that a perfect lens would pose, namely that fields (when calculated in frequency domain) would unphysically diverge in some regions of space. This issue is subsequently addressed in section 4, namely by considering the fact that all real materials are non-homogeneous (at some length scale), lossy, and divergences only occur at $t = \infty$, curtailing the unphysical divergences. Finally, we also examine how losses in general affect the performance of a super phase array, namely that losses in the NRIM would destroy the non-impact rays with the largest impact parameter first followed by impact rays. Nevertheless, even with moderate losses, it has been shown that a super phase array has better directivity and focusing power than a normal phase array (of the same physical extent).

Appendix

The scattering coefficients of (10)–(12) are given by

$$\begin{aligned}
a_m &= \frac{C_1C_2 - C_3C_4}{C_2C_5 - C_4C_6} \cdot I_m, \\
b_m &= \frac{2\mathrm{i}}{\pi} \cdot \frac{1}{k_3r_3} \cdot \frac{C_2}{C_2C_5 - C_4C_6} \cdot I_m, \\
c_m &= -\frac{2\mathrm{i}}{\pi} \cdot \frac{1}{k_3r_3} \cdot \frac{C_4}{C_2C_5 - C_4C_6} \cdot I_m, \\
d_m &= \left(\frac{2\mathrm{i}}{\pi}\right)^2 \cdot \frac{1}{k_2r_2} \cdot \frac{1}{k_3r_3} \cdot \frac{1}{C_2C_5 - C_4C_6} \cdot I_m,
\end{aligned} \tag{A.1}$$

where I_m is given by (14) and the constants C_1 to C_6 are given by:

$$\begin{aligned}
C_1 &= H_m^{(1)}(k_2r_1)H_m^{(1)\prime}(k_3r_3) - H_m^{(1)}(k_3r_3)H_m^{(1)\prime}(k_2r_1), \\
C_2 &= J_m(k_2r_2)H_m^{(1)\prime}(k_1r_2) - H_m^{(1)}(k_1r_2)J_m'(k_2r_2), \\
C_3 &= J_m(k_2r_1)H_m^{(1)\prime}(k_3r_3) - H_m^{(1)}(k_3r_3)J_m'(k_2r_1), \\
C_4 &= H_m^{(1)}(k_2r_2)H_m^{(1)\prime}(k_1r_2) - H_m^{(1)}(k_1r_2)H_m^{(1)\prime}(k_2r_2), \\
C_5 &= J_m(k_3r_3)H_m^{(1)\prime}(k_2r_1) - H_m^{(1)}(k_2r_1)J_m'(k_3r_3), \\
C_6 &= J_m(k_3r_3)J_m'(k_2r_1) - J_m(k_2r_1)J_m'(k_3r_3),
\end{aligned} \tag{A.2}$$

where the wavevectors k_1 to k_3 are given by (13) and $r_1 = r_2^2/r_3$.

References

[1] Pendry J B and Ramakrishna S A 2003 Focussing light using negative refraction *J. Phys.: Condens. Matter* **15** 6345–64

[2] Wee W H and Pendry J B 2009 Shrinking optical devices *New J. Phys.* **11** 73033–56

[3] Yang T, Chen H, Luo X and Ma H 2008 Superscatterer: enhancement of scattering with complementary media *Opt. Express* **16** 18545–50

[4] Ward A J and Pendry J B 1996 Refraction and geometry in Maxwell's equations *J. Mod. Opt.* **43** 773–93

[5] Shurig D, Pendry J B and Smith D R 2006 Calculation of material properties and ray tracing in transformation media *Opt. Express* **14** 9794–804

[6] Leonhardt U and Philbin T G 2006 General relativity in electrical engineering *New J. Phys.* **8** 247

[7] Leonhardt U and Philbin T G 2009 Transformation optics and the geometry of light *Prog. Opt.* **53** 69–152

[8] Pendry J B 2000 Negative refraction makes a perfect lens *Phys. Rev. Lett.* **85** 3966–9

[9] Pendry J B and Ramakrishna S A 2002 Near field lenses in two dimensions *J. Phys.: Condens. Matter* **14** 8463–79

[10] Pendry J B 2003 Perfect cylindrical lenses *Opt. Express* **11** 755–60

[11] Nicorovici N A, McPhedran R C and Milton G W 1994 Optical and dielectric properties of partially resonant composites *Phys. Rev.* B **49** 8479–82

[12] Nicorovici N A, Milton G W, McPhedran R C and Botten L C 2007 Quasistatic cloaking of two-dimensional polarizable discrete systems by anomalous resonance *Opt. Express* **15** 6314–23

[13] Nicorovici N A, McPhedran R C, Enoch S and Tayeb G 2008 Finite wavelength cloaking by plasmonic resonance *New J. Phys.* **10** 115020

[14] Arfken G B and Weber H J 2005 *Mathematical Methods For Physicists* 6th edn (New York: Academic)

[15] Maystre D, Enoch S and McPhedran R 2008 Why a harmonic solution for lossless, perfectly homogeneous, left-handed material cannot exist *J. Opt. Sci.* A **25** 1937–43

[16] Merlin R 2004 Analytical solution of the almost-perfect-lens problem *Appl. Phys. Lett.* **84** 1290–2

[17] Milton G W, Nicorovici N P, McPhedran R C and Podolskiy V A 2005 A proof of superlensing in the quasistatic regime and the limitations of superlenses in this regime due to anomalous localized resonance *Proc. R. Soc.* A **461** 3999–4034

[18] Gomez Santos G 2003 Universal features of the time evolution of evanescent modes in a left-handed perfect lens *Phys. Rev. Lett.* **90** 077401